Inorg. Chem. **2008**, *47*, 10744−10752

Conformation Changes and Luminescent Properties of Au-Ln (Ln = Nd, Eu, Er, Yb) Arrays with 5-Ethynyl-2,2′-Bipyridine

Hai-Bing Xu,[†] Li-Yi Zhang,[†] Jun Ni,[†] Hsiu-Yi Chao,[§] and Zhong-Ning Chen*[,†,‡]

State Key Laboratory of Structural Chemistry, Fujian Institute of Research on the Structure of Matter, Chinese Academy of Sciences, Fuzhou, Fujian 350002, China, State Key Laboratory of Organometallic Chemistry, Shanghai Institute of Organic Chemistry, Chinese Academy of Sciences, Shanghai 200032, China, and MOE Laboratory of Bioinorganic and Synthetic Chemistry, School of Chemistry and Chemical Engineering, Sun Yat-Sen University, Guangzhou, Guangdong 510275, China

Received April 24, 2008

Reaction of polymeric gold(I) acetylide species $(bpyC{\equiv}CAu)_n$ (bpyC≡CH = 5-ethynyl-2,2′-bipyridine) with diphosphine ligands $Ph_2P(CH_2)_nPPh_2$ ($n = 2-6$) or 1,1′-bis(diphenylphosphino)-ferrocene (dppf) in dichloromethane induces isolation of binuclear gold(I) complexes $(bpyC{\equiv}CAu)_2\{\mu\text{-}Ph_2P(CH_2)_nPPh_2\}$ or $(bpyC{\equiv}CAu)_2(\mu\text{-dppf})$. Complexation of $Ln(hfac)_3$ (hfac = hexafluoroacetylacetonate, Ln = Nd, Eu, Er, Yb) subunits to the binuclear gold(I) complexes through 2,2′-bipyridyl chelation gives the corresponding Au_4Ln_4 or Au_2Ln_2 heteropolynuclear complexes. Noticeably, upon formation of the Au_4Ln_4 arrays by complexation of $(bpyC{\equiv}CAu)_2(\mu\text{-}Ph_2P(CH_2)_4PPh_2)$ (**3**) with $Ln(hfac)_3$ units, trans-conformation in **3** transforms dramatically to the cis-arranged form due to the strong driving force from ligand-unsupported Au−Au contacts between two Au_2Ln_2 subunits. In contrast, cis-conformation in $(bpyC{\equiv}CAu)_2(\mu\text{-dppf})$ (**6**) stabilized by Au−Au interactions is reversed to the trans-oriented form upon formation of Au_2Ln_2 arrays by introducing $Ln(hfac)_3$ units through 2,2-bipyridyl chelation. The binuclear gold(I) complexes show bright blue luminescence featured by ligand-centered $\pi \rightarrow \pi^*$ (C≡Cbpy) states together with low-energy emission at 500−540 nm, associated with $^3(\pi{\rightarrow}\pi^*)$ excited states, mixed probably with some characteristic from (Au−Au) → (C≡Cbpy) ^{3}MMLCT transition. For Au_4Ln_4 or Au_2Ln_2 complexes, sensitized lanthanide luminescence is achieved by energy transfer from Au-acetylide chromophores with lifetimes in the sub-millisecond range for Eu^{III} complexes, whereas in the microsecond range for near-infrared emitting Nd^{III}, Er^{III}, and Yb^{III} species.

Introduction

Lanthanide(III) compounds that exhibit typical narrow bandwidth emissions have extensive applications in many fields including light-emitting devices, light amplifiers and biological assays, etc.[1] Traditionally, luminescence from lanthanide ions is achieved by excitation of strongly absorbing organic ligands bound directly to the lanthanide centers.[1a] A new approach to achieve long-lived lanthanide emission has been recently established by effective energy transfer from d-block organometallic chromophores.[2−8] Particularly, sensitized lanthanide luminescence is successfully achieved by energy transfer from platinum(II) alkynyl chromophores to lanthanide centers in a series of Pt-Ln bimetallic polynuclear complexes using polypyridyl-functionalized acetylides as bifunctional bridging ligands,

* To whom correspondence should be addressed. E-mail: czn@fjirsm.ac.cn.
† Fujian Institute of Research on the Structure of Matter.
‡ Shanghai Institute of Organic Chemistry.
§ Sun Yat-Sen University.

(1) (a) Bünzli, J.-C. G.; Piguet, C. *Chem. Soc. Rev.* **2005**, *34*, 1048. (b) Kang, T. S.; Harrison, B. S.; Bouguettaya, M.; Foley, T. J.; Boncella, J. M.; Schanze, K. S.; Reynolds, J. Y. *Adv. Funct. Mater.* **2003**, *13*, 205. (c) Suzuki, H. J. *Photochem. Photobiol. A.* **2004**, *166*, 155. (d) Kawamura, Y.; Wada, Y.; Hasegawa, Y.; Iwamuro, M.; Kitamura, T.; Yanagida, S. *Appl. Phys. Lett.* **1999**, *74*, 3245.
(2) (a) Klink, S. I.; Keizer, H.; van Veggle, F. C. J. M. *Angew. Chem., Int. Ed.* **2000**, *39*, 4319. (b) Coppo, P.; Duati, M.; Kozhevnikov, V. N.; Hofstraat, J. W.; Cola, L. D. *Angew. Chem.Int. Ed.* **2005**, *44*, 1806.
(3) (a) Imbert, D.; Cantuel, M.; Bünzli, J.-C. G.; Bernardinelli, G.; Piguet, C. J. *Am. Chem. Soc.* **2003**, *125*, 15698. (b) Pope, S. J. A.; Coe, B. J.; Faulkner, S.; Bichenkova, E. V.; Yu, X.; Douglas, K. T. J. J. *Am. Chem. Soc.* **2004**, *126*, 9490.
(4) Ward, M. D. *Coord. Chem. Rev.* **2007**, *251*, 1663.
(5) (a) Chen, F.-F.; Bian, Z.-Q.; Liu, Z.-W.; Nie, D.-B.; Chen, Z.-Q.; Huang, C.-H. *Inorg. Chem.* **2008**, *47*, 2507. (b) Beer, P. D.; Szemes, F.; Passaniti, P.; Maestri, M. *Inorg. Chem.* **2004**, *43*, 3965. (c) Sanada, T.; Suzuki, T.; Yoshida, T.; Kaizaki, S. *Inorg. Chem.* **1998**, *37*, 4712.

10.1021/ic800733x CCC: $40.75
Published on Web 10/22/2008

where the "soft" acetylide C donors are bound to platinum(II) subunits and "hard" polypyridyl N donors associated with lanthanide centers.[6,7]

Recent interest in gold(I) alkynyl complexes have primarily focused on their rich structural topology, intriguing photoluminescence and photochemical properties.[9−11] By modification of steric effects and electronic properties of the alkynyl ligands, gold(I) alkynyl complexes with a wide range of structural topologies are accessible.[12] Gold(I) alkynyl complexes of phosphines with two-coordinated geometry frequently exhibit short gold(I)−gold(I) contacts, inducing a wide range of molecular structures with various topologies.[13,14] These gold(I) alkynyl phosphine species are usually room-temperature luminescent, arising from intraligand $\pi \rightarrow \pi^*$ (C≡C−R), ^{3}[(x2)σ(Au−P) → π^*(C≡C−R)] (MLCT), and/or ^{3}[(x2)dσ^*(Au−Au) → π^*(C≡C−R)] MMLCT (metal−metal-to-ligand charge-transfer) transitions.[9−12,15] It is anticipated that these Au^I acetylide phosphine chromophores are likely favorable antenna chromophores for sensitization of lanthanide luminescence. In view of the structural flexibility in gold(I) alkynyl diphosphine complexes, incorporating $Ln(hfac)_3$ subunits to these gold(I) species with polypyridyl-functionalized alkynyl ligands induces intriguing conformational changes in the gold(I) alkynyl diphosphine subunits and thus formation of Au^I-Ln^{III} arrays with various structural topologies. By this consideration, a series of binuclear gold(I) alkynyl complexes of diphosphines were prepared by depolymerization of polymeric $(bpyC{\equiv}CAu)_n$ using diphosphines $Ph_2P(CH_2)_nPPh_2$ or 1,1′-bis(diphenylphosphino)-ferrocene (dppf). Reactions of these binuclear gold(I) alkynyl diphosphine complexes with $Ln(hfac)_3(H_2O)_2$ (Ln = Nd, Eu, Er, Yb) caused isolation of a series of Au^I-Ln^{III} arrays with dramatic cis−trans conformation transformations in the gold(I) alkynyl subunits, in which sensitized lanthanide luminescence occurs indeed by energy transfer from the gold(I) alkynyl chromophores.

Results and Discussion

Syntheses and Characterization. 1−6 were isolated from the reaction of $Ph_2P(CH_2)_nPPh_2$ ($n = 2-6$) or dppf with 2 equiv of $(bpyC{\equiv}CAu)_n$ in dichloromethane solutions. The acetylides are σ-bonded to gold(I) centers, whereas the 2,2′-bipyridyl is free of coordination in these binuclear gold(I) complexes. In order to access Au-Ln heteronuclear arrays by complexation of $Ln(hfac)_3$ subunits with binuclear gold(I) moieties through 2,2′-bipyridyl chelating, reactions of **3** or **6** with 2.2 equiv of $Ln(hfac)_3(H_2O)_2$ (Ln = Nd, Eu, Er, and Yb) in dichloromethane induced formation of the corresponding Au-Ln complexes **7−10** or **11−14** as depicted in Scheme 1.

These complexes were characterized by elemental analyses, IR spectra, ^{1}H and ^{31}P NMR spectroscopy and/or ESI-MS spectrometry. For binuclear gold(I) alkynyl diphosphines complexes **1−6**, positive ion ESI-MS revealed that molecular ion fragments $[M + H]^+$, and/or $[M - (bpyC{\equiv}C)]^+$ occur as the base peaks or principal peaks with high abundance. The ^{31}P NMR spectra show one singlet for $Ph_2P(CH_2)_nPPh_2$ or dppf in these complexes, indicating the equivalence of P donors in **1−6** on NMR time-scale.

Slow diffusion of *n*-hexane into the concentrated dichloromethane solutions of **1**, **3**, **6**, **9** and **13** afforded pale yellow crystals suitable for X-ray diffraction measurements. Selected bonding lengths and angles are presented in Table 1. ORTEP drawings of **1**, **3**, **6**, **9** and **13** are depicted in Figures 1–5, respectively. The gold(I) coordination geometry is quasi-linear with the C−Au−P angles in the range 171.4(2)−177.2(3)°. The Au−P bond distances (2.268(2)−2.281(2) Å) are comparable to those in the gold(I) arylacetylide complexes (2.263(3)−2.277(1) Å) with PPh_3 ligands,[10b,16] but longer than those in the gold(I) chloride phosphine complexes.[17] The Au−C (1.979(1)−2.242(1) Å) and C≡C (1.159(5)−1.219(2) Å) distances are also similar to those in the analogous gold(I) arylacetylide complexes.[9b,10c,d,16b,18,19]

In contrast to the *trans*-oriented binuclear gold(I) units in both **1** (Figure 1) and **3** (Figure 2), the binuclear gold(I) moiety in **6** (Figure 3) is *cis*-arranged, in which the short

(6) (a) Xu, H.-B.; Shi, L.-X.; Ma, E.; Zhang, L.-Y.; Wei, Q.-H.; Chen, Z.-N. *Chem. Commun.* **2006**, 1601. (b) Xu, H.-B.; Zhang, L.-Y.; Xie, Z.-L.; Ma, E.; Chen, Z.-N. *Chem. Commun.* **2007**, 2744. (c) Xu, H.-B.; Zhang, L.-Y.; Chen, Z.-H.; Si, L.-X.; Chen, Z.-N. *Dalton Trans.* **2008**, 4664. (d) Li, X.-L.; Dai, F.-R.; Zhang, L.-Y.; Zhu, Y.-M.; Peng, Q.; Chen, Z.-N. *Organometallics* **2007**, *26*, 4483. (e) Li, X.-L.; Shi, L.-X.; Zhang, L.-Y.; Wen, H.-M.; Chen, Z.-N. *Inorg. Chem.* **2007**, *46*, 10892. (f) Xu, H.-B.; Ni, J.; Chen, K.-J.; Zhang, L.-Y.; Chen, Z.-N. *Organometallics*, in press (DOI: 10.1021/OM8005883).

(7) (a) Ronson, T. K.; Lazarides, T.; Adams, H.; Pope, S. J. A.; Sykes, D.; Faulkner, S.; Coles, S. J.; Hursthouse, M. B.; Clegg, W.; Harrington, R. W.; Ward, M. D. *Chem. Eur. J.* **2006**, *12*, 9299. (b) Ziessel, R.; Diring, S.; Kadjane, P.; Charbonnière, L.; Retailleau, P.; Philouze, C. *Chem. Asian J.* **2007**, *2*, 975.

(8) (a) Rawashdeh-Omary, M. A.; Larochelle, C. L.; Patterson, H. H. *Inorg. Chem.* **2000**, *39*, 4527. (b) Beeby, A.; Dickins, R. S.; FitzGerald, S.; Govenlock, L. J.; Maupin, C. L.; Parker, D.; Riehl, J. P.; Siligardi, G.; Williams, J. A. G. *Chem. Commun.* **2000**, 1183. (c) Glover, P. B.; Ashton, P. R.; Childs, L. J.; Rodger, A.; Kercher, M.; Williams, R. M.; De Cola, L.; Pikramenou, Z. *J. Am. Chem. Soc.* **2003**, *125*, 9918.

(9) (a) Yam, V. W.-W.; Choi, S. W.-K.; Cheung, K.-K. *Organometallics* **1996**, *15*, 1734. (b) Yam, V. W.-W.; Choi, S. W. K. *J. Chem. Soc., Dalton Trans.* **1996**, 4227.

(10) (a) Irwin, M. J.; Vittal, J. J.; Puddephatt, R. J. *Organometallics* **1997**, *16*, 3541. (b) Irwin, M. J.; Rendina, L. M.; Vittal, J. J.; Puddephatt, R. J. *Chem. Commun.* **1996**, 1281. (c) Jia, G.; Puddephatt, R. J.; Scott, I. D.; Vittal, J. J. *Organometallics* **1993**, *12*, 3565. (d) Irwin, M. J.; Jia, G.; Payne, N. C.; Puddephatt, R. J. *Organometallics* **1996**, *15*, 51.

(11) (a) Puddephatt, R. J. *Chem. Commun.* **1998**, 1055. (b) Mingos, D. M. P.; Yau, J.; Menzer, S.; Williams, D. J. *Angew. Chem., Int. Ed.* **1995**, *34*, 1894.

(12) McArdle, C. P.; Jennings, M. C.; Vittal, J. J.; Puddephatt, R. J. *Chem. Eur. J.* **2001**, *7*, 3572.

(13) Puddephatt, R. J. *Comprehesive Coordination Chemistry*; Wilkinson, G., Gillard, R. D., McCleverty, J. A., Eds.; Pergamon: Oxford, 1987; Vol. 5, p 861.

(14) Grohmann, A.; Schmidbaur H. *Comprehensive Organometallic Chemistry II*; Abel, E. W. Stone, F. G. A. Wilkinson G., Eds; Pergamon: Oxford, 1995; Vol. 3, p 1.

(15) Long, N. J.; Williams, C. K. *Angew. Chem., Int. Ed.* **2003**, *42*, 2586.

(16) (a) Yam, V. W.-W.; Lee, W. K.; Lai, T. F. *Organometallics* **1993**, *12*, 2197. (b) Whittall, R. I.; Humphrey, M. G.; Houbrechts, S.; Persoons, A.; Hockless, D. C. R. *Organometallics* **1996**, *15*, 5738.

(17) (a) Angwemaier, K.; Zeller, E.; Schmidbaur, H. J. *Organomet. Chem.* **1994**, *472*, 371. (b) Assefa, Z.; McBurnett, B. G.; Staples, R. J.; Fackler, J. P.; Assmann, B.; Angermaier, K.; Schmidbaur, H. *Inorg. Chem.* **1995**, *34*, 75.

(18) MacDonald, M.-A.; Puddephatt, R. J.; Glenn, P. A. Y. *Organometallics* **2000**, *19*, 2194.

(19) (a) Li, D.; Hong, X.; Che, C.-M.; Lo, W.-C.; Peng, S.-M. *J. Chem. Soc., Dalton Trans.* **1993**, 2929. (b) Tzeng, B. C.; Lo, W.-C.; Che, C.-M.; Peng, S. M. *Chem. Commun.* **1996**, 181. (c) Xiao, H.; Cheung, K. K.; Che, C.-M. *J. Chem. Soc., Dalton Trans.* **1996**, 3699.

Scheme 1. Synthetic Routes to the Au-Ln Heteronuclear Complexes **7**−**14**

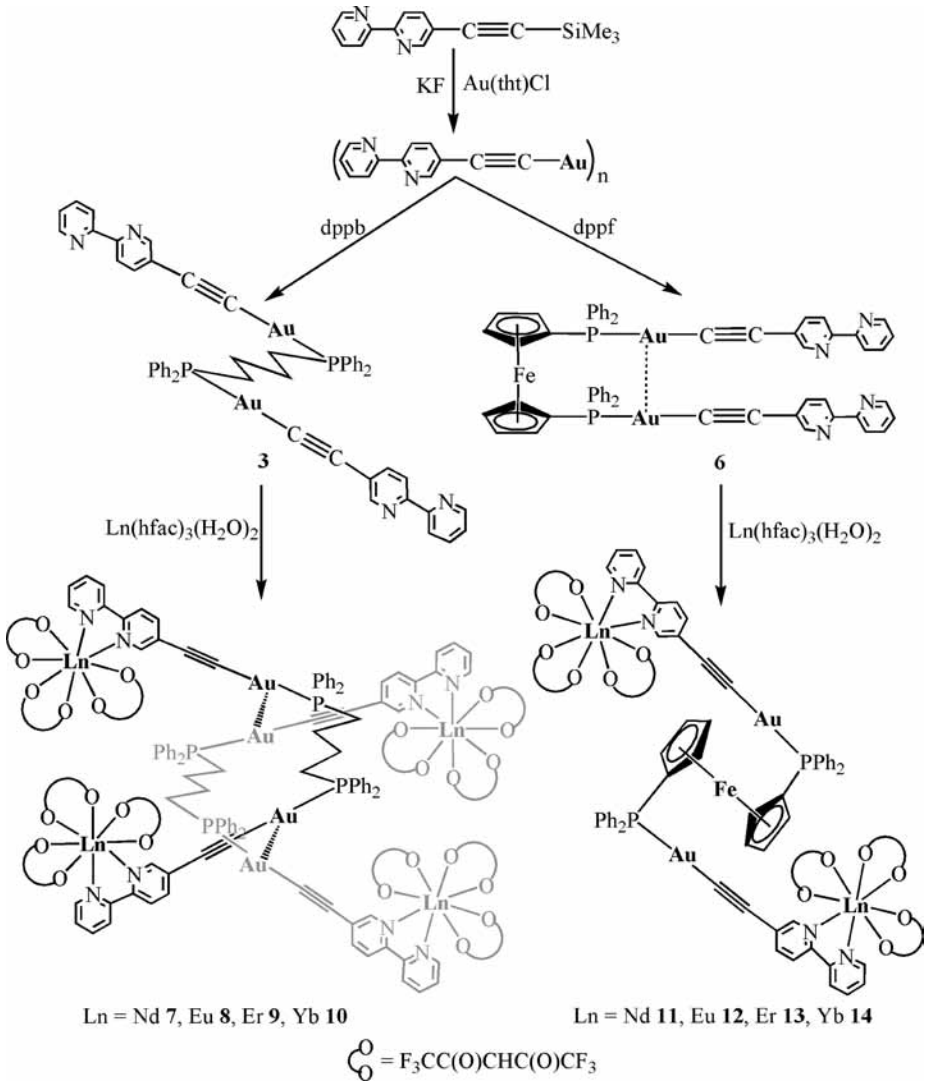

Table 1. Selected Bond Distances (Å) and Angles (°) for Compounds **1**·2CH_2Cl_2, **3**·H_2O, **6**·CH_2Cl_2, **9**·H_2O, and **13**·2H_2O

1·2CH_2Cl_2		**3**·H_2O		**6**·CH_2Cl_2		**9**·H_2O		**13**·2H_2O	
C1−C2	1.167(9)	C10−C11	1.206(2)	C1−C2	1.203(1)	C1−C2	1.219(2)	C1−C2	1.207(1)
C3−C4	1.170(9)	C30−C31	1.159(5)			C3−C4	1.173(2)		
Au1−C1	2.014(6)	Au1−C10	2.131(8)	Au1−C1	1.984(7)	Au1−C1	1.979(1)	Au1−C1	1.985(8)
Au2−C3	2.017(6)	Au2−C30	2.242(1)			Au2−C3	2.008(1)		
Au1−P1	2.274(2)	Au1−P1	2.268(2)	Au1−P1	2.271(2)	Au1−P1	2.276(3)	Au1−P1	2.281(2)
Au2−P2	2.272(2)	Au2−P2	2.272(2)			Au2−P2	2.280(4)		
Au1...Au2	3.0692(5)			Au1...Au1A	3.2555(7)	Au1...Au2	3.1329(1)		
C1−Au1−P1	172.3(3)	C10−Au1−P1	175.6(3)	C1−Au1−P1	171.4(2)	C1−Au1−P1	175.0(4)	C1−Au1−P1	174.3(3)
C3−Au2−P2	173.0(2)	C30−Au2−P2	177.2(3)			C3−Au2−P2	172.2(4)		
C2−C1−Au1	176.0(9)	C11−C10−Au1	161.8(1)	C2−C1−Au1	168.8(7)	C2−C1−Au1	172.6(1)	C2−C1−Au1	172.8(8)
C4−C3−Au2	170.5(8)	C31−C30−Au2	162(2)			C4−C3−Au2	174.0(1)		
C1−C2−C14	176.0(1)	C10−C11−C12	177.8(2)	C1−C2−C14	176.8(9)	C1−C2−C15	175.5(2)	C1−C2−C15	176.1(1)
C3−C4−C34	174.0(1)	C30−C31−C32	162(2)			C3−C4−C35	171.1(2)		

intramolecular Au−Au (3.26 Å) contact in **6** is a direct driven force for formation of the *cis*-arranged conformation. Interestingly, short Au−Au contacts (3.07 Å) exist between binuclear gold(I) subunits in **1** so as to form a ribbon structure through ligand-unsupported Au−Au interaction as depicted in Figure 1. The two C≡Cbpy in a binuclear gold(I) moiety are coplanar in **3**, but form a dihedral angle of 78.5° for **1** and 57.5° for **6** between the two least-squares planes.

The heterooctanuclear Au_4Er_4 array in **9** (Figure 4) originates from incorporating two binuclear gold(I) moiety **3** with four Er(hafc)$_3$ units through 2,2-bipyridyl chelation to the Er^{III} centers, where the Au_4Er_4 array consists of two Au_2Er_2 subunits associated with each other through ligand-unsupported Au−Au interactions (Au−Au = 3.13 and 3.22 Å). As depicted in Figure 4, the [Au{P$(CH_2)_4$P}Au]$_2$ moiety forms a 16-membered ring owing to the presence of Au−Au interactions between two Au{P$(CH_2)_4$P}Au subunits. It is noteworthy that upon formation of the Au_4Er_4 array, *trans*-arranged binuclear gold(I) unit in the precursor complex **3** (Figure 2) is converted into *cis*-conformation in **9** (Figure

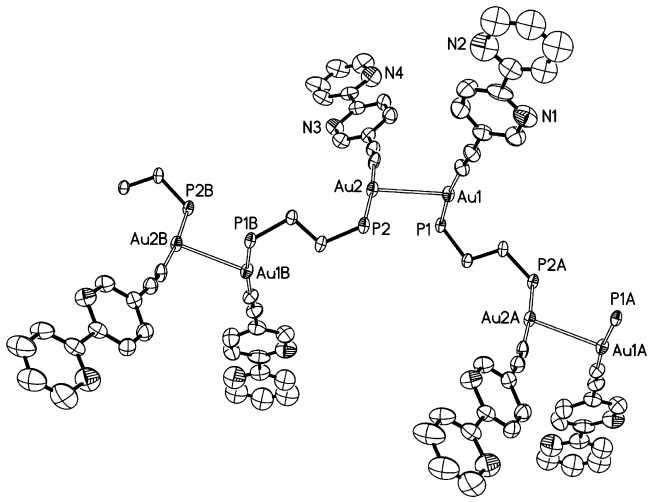

Figure 1. ORTEP drawing of **1** with atom labeling scheme showing 30% thermal ellipsoids. Phenyl rings on the phosphorus atoms are omitted for clarity.

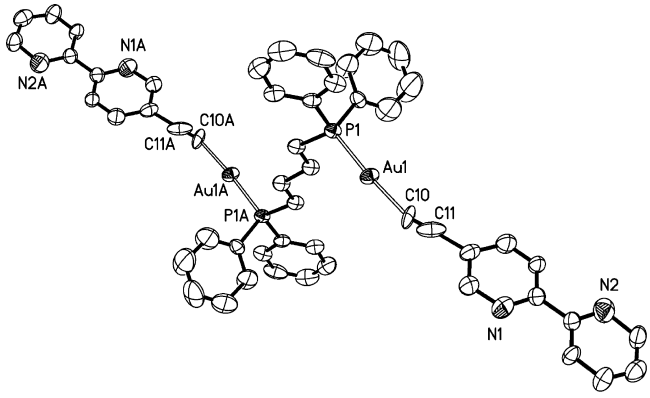

Figure 2. ORTEP drawing of **3** with atom labeling scheme showing 30% thermal ellipsoids.

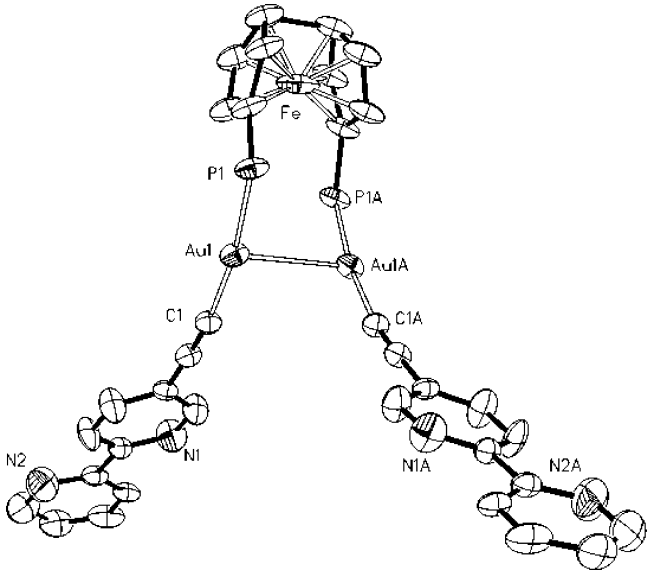

Figure 3. ORTEP drawing of **6** with atom labeling scheme showing 30% thermal ellipsoids. Phenyl rings on the phosphorus atoms are omitted for clarity.

4). Undoubtedly, the trans → cis transformation from **3** to **9** is a direct consequence due to formation of strong ligand-unsupported Au−Au contacts between two Au_2Er_2 subunits

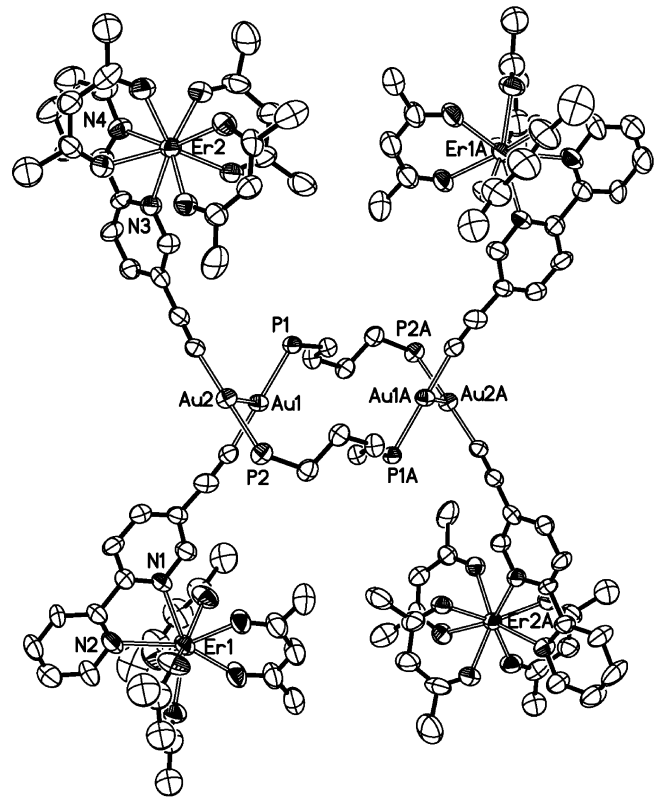

Figure 4. ORTEP drawing of **9** with atom labeling scheme showing 30% thermal ellipsoids. Phenyl rings on the phosphorus atoms and the F atoms on the trifluoromethyl are omitted for clarity.

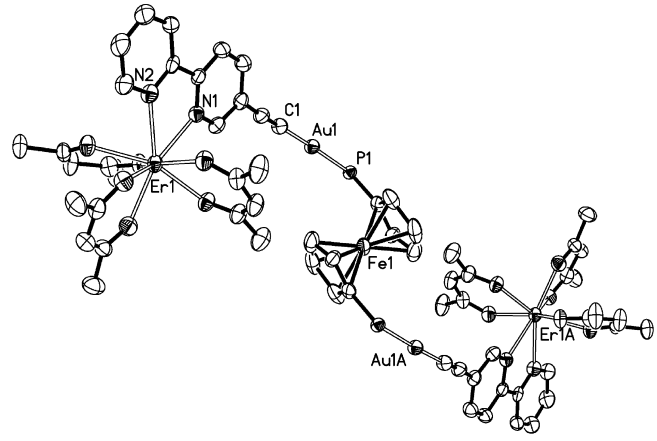

Figure 5. ORTEP drawing of **13** with atom labeling scheme showing 30% thermal ellipsoids. Phenyl rings on the phosphorus atoms and the F atoms on the trifluoromethyl are omitted for clarity.

in the Au_4Er_4 array. The gold(I) center is quasi-linearly coordinated by diphosphine P and acetylide C donors with P−Au−C angles being 172.2(4)° and 175.0(4)°, comparable to those found in the binuclear gold(I) complex **3** (175.6(3)° and 177.2(3)°). The Er^{III} center is eight-coordinated with N_2O_6 donors to form a distorted square antiprism as found in a series of Pt-Ln heteronuclear arrays.[6,7,20,21] The Au···Er separations through bridging 5-ethynyl-2,2′-bipyridine are 8.25 and 8.77 Å.

In contrast, upon formation of Au_2Er_2 array in **13** (Figure 5) by incorporating **6** (Figure 3) with $Er(hfac)_3$ unit, *cis*-arranged binuclear gold(I) unit in **6** is transformed into *trans*-

Table 2. UV-vis Absorption and Luminescence Data for **1**−**14**

complex	medium (T/K)	λ_{abs}/nm (ε/dm^3 mol^{-1} cm^{-1})	λ_{em}/nm (τ /μs)	Φ_{em}
1	CH_2Cl_2 (298)	230(60570), 317(70610), 329(66000), 344sh(8310)	399(2.2 ns)	0.16[b]
	CH_2Cl_2 (77)		498(max), 540	
	solid (298)		420(0.28 ns), 500(3.2 ns), 545(2.6 ns)	
	solid (77)		501(max), 540	
2	CH_2Cl_2(298)	230(61390), 317(86310), 330(81460), 342sh(15600)	399(2.1 ns)	0.17[b]
	CH_2Cl_2(77)		498(max), 540	
	solid(298)		425(0.45 ns), 502(2.2 ns), 540(2.3 ns)	
	solid(77)		422, 501, 540	
3	CH_2Cl_2(298)	229(53020), 318(85680), 330(85950), 344sh(19600)	399(2.1 ns)	0.13[b]
	CH_2Cl_2(77)		498(max), 540	
	solid(298)		424(0.36 ns), 541(2.2 ns)	
	solid(77)		423(max), 522	
4	CH_2Cl_2(298)	230(74830), 317(103420), 330(96630), 344sh(10800)	399(2.3 ns)	0.30[b]
	CH_2Cl_2(77)		498(max), 540	
	solid(298)		423(0.43 ns), 542(2.4 ns)	
	solid(77)		423(max), 537	
5	CH_2Cl_2(298)	230 (57240), 317 (83760), 330 (79110), 344sh (8100)	399(1.8 ns)	0.26[b]
	CH_2Cl_2(77)		498(max), 540	
	solid(298)		438(0.43 ns), 553(2.4 ns)	
	solid(77)		425(max), 543	
6	CH_2Cl_2(298)	229(67370), 318(77830), 330(73870), 344sh(14130)	nonemissive	
7	CH_2Cl_2(298)	229(68300), 304(96100), 329sh (70380), 355sh(67800)	1057(weak)	
	solid(298)		1057(weak)	
8	CH_2Cl_2(298)	228(89140), 302(137910), 328sh(100270), 354sh(91240)	613 (557)	0.012[c]
	solid(298)		613 (587.9)	
9	CH_2Cl_2(298)	229(80060), 300(135380), 328 (sh, 81420), 353sh(73200)	1535(weak)	
	solid(298)		1535(weak)	
10	CH_2Cl_2(298)	235(103950), 304(135300), 332sh(67550), 357sh(58060)	980(11.9)[a]	0.006[d]
	solid(298)		980(14.6)[a]	
11	CH_2Cl_2(298)	228(50450), 304(74190), 330sh(47760), 352sh(28190)	1057(weak)	
	solid(298)		1057(weak)	
12	CH_2Cl_2(298)	229(78170), 303(98450), 331sh(65800), 353sh(48400)	613(204.5)	0.01[c]
	solid(298)		613(102.5)	
13	CH_2Cl2(298)	229(65330),301(69970), 329sh (42400), 354sh(27300)	1535(weak)	
	solid(298)		1535(weak)	
14	CH_2Cl_2(298)	228(75500), 295(135200), 330sh(51420), 354sh(14470)	980(11.9)[a]	0.006[d]
	solid(298)		980(14.4)[a]	

[a] The excitation wavelength in the lifetime measurement is 397 nm. [b] The quantum yield of binuclear gold(I) complexes in degassed dichloromethane was determined relative to that of $Cy_3PAuC{\equiv}CPh$ ($\Phi = 0.08$)[22] in degassed dichloromethane. [c] The quantum yields of Eu^{III} complexes in degassed dichloromethane are determined relative to that of $Ru(bpy)_3(PF_6)_2$ ($\Phi = 0.064$)[26] in degassed acetonitrile. [d] The quantum yield of Yb complexes in dichloromethane solutions is estimated by the equation $\Phi_{Ln} = \tau_{obs}/\tau_0$, in which τ_{obs} is the observed emission lifetime and τ_0 is the radiative or "natural" lifetime with $\tau_0 = 2$ ms.[21a,b]

oriented form in **13** as indicated in Scheme 1. Obviously, introducing the $Er(hfac)_3$ unit to the binuclear gold(I) species through 2,2′-bipyridyl chelation induces breaking of the Au−Au contact in the precursor species **6**, and thus cis → trans conversion from **6** to **13**. Although two C≡Cbpy in the binuclear gold(I) unit form a dihedral angle of 57.5° in **6** between two least-squares planes, they become coplanar in **13** upon formation of Au_2Er_2 array accompanying by cis → trans conformational conversion. The Au···Er separation through bridging 5-ethynyl-2,2′-bipyridine is 8.55 Å in **13**, comparable to that found in the Au_4Er_4 complex **9**. Likewise, the gold(I) atoms adopt a quasi-linear coordination environment with CP donors and Er^{III} centers are eight-coordinated with N_2O_6 chromophore to afford a distorted square antiprismatic geometry.

UV−vis Absorption Properties. The UV−vis absorption spectral data of **1**−**14** are summarized in Table 2. The diphosphine-linked binuclear gold(I) complexes **1**−**6** exhibit three distinct absorption bands with the maxima at ca. 230, 320, and 345(sh) nm, independent of the spacer between two P donors in the diphosphine. For the purpose of comparison so as to elucidate the absorption feature of binuclear gold(I) precursor species and their corresponding gold(I)-lanthanide(III) heteronuclear complexes, the absorption spectra of Au_2 complex **3**, Au_4Er_4 species **9**, $bpyC{\equiv}CSiMe_3$ and model compound $Er(hfac)_3(bpyC{\equiv}CSiMe_3)$ in dichloromethane solutions are depicted in Figure 6. The UV−vis spectra of both $bpyC{\equiv}CSiMe_3$ and $Er(hfac)_3(bpyC{\equiv}CSiMe_3)$ show intense absorption bands at ca. 300−320 nm due to $\pi \rightarrow \pi^*$ transitions from the alkynyl ligands or hexafluoroacetylacetonate.[6,7] As shown in Figure 6, three absorption maxima are observed at 317, 330, 344 nm in the UV−vis spectrum of binuclear gold(I) complex **3**, which are obviously red-shifted compared to those of the free ligand $bpyC{\equiv}CSiMe_3$. The spacings between three maxima at 317−344 nm are 1242 and 1233 cm^{-1}, corresponding to vibrational stretching frequencies of the pyridyl in 5-ethynyl-2,2′-bipyridine.[22] On the basis of related comparison together with reference to the assignment on a series of platinum(II) phospine alkynyl

(20) Chen, Z. N.; Fan, Y.; Ni, J. *Dalton Trans.* **2008**, 573.
(21) (a) Shavaleev, N. M.; Moorcraft, L. P.; Pope, S. J. A.; Bell, Z. R.; Faulkner, S.; Ward, M. D. *Chem. Commun.* **2003**, 1134. (b) Shavaleev, N. M.; Moorcraft, L. P.; Pope, S. J. A.; Bell, Z. R.; Faulkner, S.; Ward, M. D. *Chem. Eur. J.* **2003**, *9*, 5283. (c) Shavaleev, N. M.; Accorsi, G.; Virgili, D.; Bell, Z. R.; Lazarides, T.; Calogero, G.; Armaroli, N.; Ward, M. D. *Inorg. Chem.* **2005**, *44*, 61.

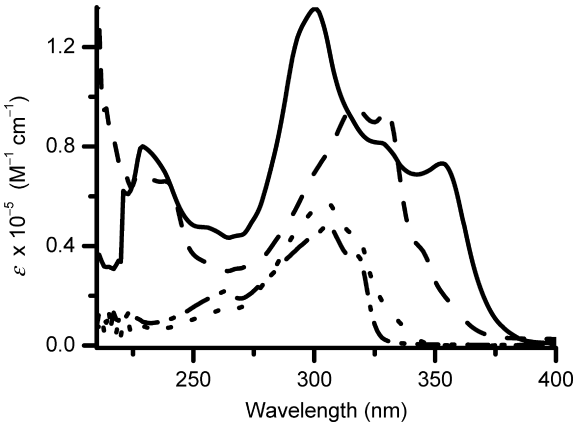

Figure 6. The UV−vis absorption spectra of **3** (dash), **9** (solid), Er(hfac)$_3$(bpyC≡CSiMe$_3$) (dot) and bpyC≡CSiMe$_3$ (dash dot).

complexes,[10b,16,19] the UV−vis absorption features of these diphosphine-linked binuclear gold(I) complexes are most likely ascribable to the alkynyl ligand-centered $^1(\pi \rightarrow \pi^*)$ states. Upon formation of Au_4Er_4 array **9**, the absorption maxima (328 and 352 nm) are distinctly red-shifted compared with those of the binuclear gold(I) precursor complex **3**. The vibrational spacing between the peak maxima 328 and 352 nm is 2079 cm^{-1} in **9**, which is typical for the ν(C≡C) stretching mode of the acetylide. Consequently, the low-energy absorption features in Au-Ln heteronuclear complexes arise from the alkynyl ligand-centered $^1(\pi \rightarrow \pi^*)$ transitions.

Luminescence Properties. The luminescence data including emission lengths, lifetimes and quantum yields of **1**−**14** are presented in Table 2. Upon excitation of **1**−**5** at λ_{ex} > 350 nm, these binuclear gold(I) species show bright blue to yellow emissions in solid states and solutions at both 298 and 77 K. The dppf-containing binuclear gold(I) species **6**, however, is nonemissive due to electron transfer quenching from the electron-rich ferrocenyl. The emission spectra of **1**−**5** in solid states at 298 K are shown in Figure 7. **1** shows intense low-energy bands at 500−540 nm together with weak a high-energy band at 420 nm. On the contrary, the intensity of high-energy bands at ca. 420 nm in the emission spectra of **2**−**5** is stronger than that of low-energy bands at 500−540 nm. Compared with the emission spectrum of bpyC≡CSiMe$_3$, the emission of binuclear gold(I) complexes **1**−**5** at ca. 420 nm is most probably from the $^1(\pi \rightarrow \pi^*)$ excited-state of the alkynyl ligand.[6] With reference to the emission properties of (R$_3$P)Au(C≡CR′) (R, R′ = alkyl or aryl)[10c,22] and (Ph$_2$P(CH$_2$)$_n$PPh$_2$){Au(C≡CR′)}$_2$ (n = 1, 2, 3)[19] together with the vibrational spacing of 1481 cm^{-1}, the emission bands at ca. 500−540 nm are tentatively assigned to the $^3(\pi \rightarrow \pi^*)$ excited-state of the acetylide ligand, mixed probably with some character from (Au−Au)→(C≡Cbpy) ^{3}MMLCT transition.[9b,15,22] In fluid dichloromethane at ambient temperature, however, **1**−**5** exhibit much stronger high-energy emission at ca. 420 nm, whereas the emission intensity of the low-energy band at ca. 500−540 nm is quite weak. In order to get deeper insight to the emissive properties of **1**−**5**, the emission spectra of solid state and frozen solution samples were measured at 77 K. Noticeably, the intensity of low-energy emission bands (500−540 nm) becomes significantly stronger than that of the high-energy emission bands (ca. 420 nm) at 77 K (Figure S3, Supporting Information). Particularly, as indicated in Figure 8, the low-energy emission bands at 500−540 nm were only observed in the emission spectra of **1**−**5**, whereas the high-energy emission bands disappeared in frozen dichloromethane at 77 K. This together with the vibronic-structured emission bands at 500 and 540 nm with the vibrational progressional spacing of 1481 cm^{-1} supports the notion that the luminescence of **1**−**5** at 77 K arises likely from the $^3(\pi \rightarrow \pi^*)$ excited states together with some character from (Au−Au) → (C≡Cbpy) ^{3}MMLCT transition.

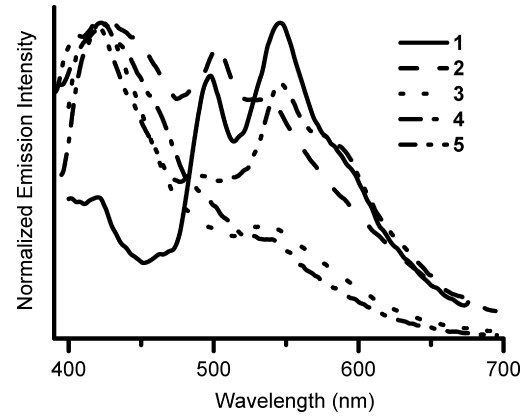

Figure 7. Emission spectra of **1**−**5** in the solid states at 298 K. Emission spectra of **1**−**5** in the solid states at ambient temperature.

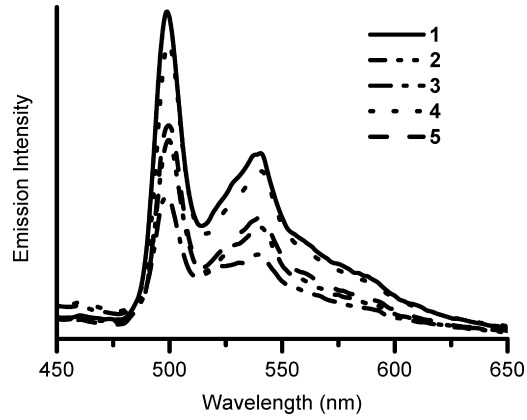

Figure 8. Emission spectra of **1**−**5** in frozen dichloromethane at 77 K.

Upon excitation of the gold(I) alkynyl chromophores with λ_{ex} > 350 nm, the Au-Ln heteropolynuclear complexes **7**−**14** show narrow bandwidth luminescence that is characteristic of the corresponding lanthanide ions with a microsecond range of lifetimes in both solid states and fluid dichloromethane at ambient temperature (Table 2). As depicted in Figure 9, typical lanthanide emission occurs in the corresponding Au_4Ln_4 (Ln = Nd, Eu, Er, and Yb) species **7**−**10**. On the contrary, the (bpyC≡CAu)$_2$(μ-dppb) chromophore-based emission in the visible region is remarkably attenuated

(22) (a) Che, C. M.; Chao, H. Y.; Miskowski, V. M.; Li, Y.; Cheung, K. K. J. *Am. Chem. Soc.* **2001**, *123*, 4985. (b) Chao, H -Y.; Lu, W.; Li, Y.; Chan, M. C. W.; Che, C.-M.; Cheung, K.-K.; Zhu, N. J. *Am. Chem. Soc.* **2002**, *124*, 14696.

(23) (a) Chan, C.-W.; Cheng, L.-K.; Che, C.-M. *Coord. Chem. Rev.* **1994**, *132*, 87. (b) Hissler, M.; McGarrah, J. E.; Connick, W. B.; Geiger, D. K.; Cummings, S. D.; Eisenberg, R. *Coord. Chem. Rev.* **2000**, *208*, 115.

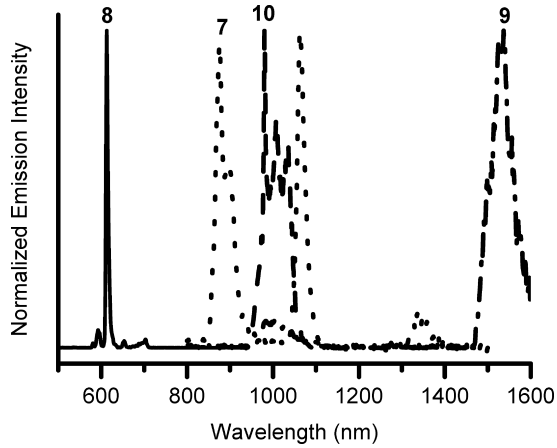

Figure 9. Emission spectra of Au-Ln complexes **7** (dot), **8** (solid), **9** (dash dot) and **10** (dash) in dichloromethane at ambient temperature. Emission spectra of Au-Ln species **7** (dot), **8** (solid), **9** (dash dot), and **10** (dash) in dichloromethane at 298 K.

in all of the Au_4Ln_4 complexes **7**−**10**, because effective energy transfer is most likely operating from Au^I alkynyl subunit to lanthanide centers through the bridging pathway Ln-bpyC≡C−Au with the Au···Ln distance being ca. 8.4 Å.[2−8] Titration of **3** with $Er(hfac)_3(H_2O)_2$ in dichloromethane solution induces rapid attenuation of the $(bpyC{\equiv}CAu)_2(\mu$-dppb) chromophore-based emission, but the high-energy emission at 380−420 nm due to the $^1(\pi \rightarrow \pi^*)$ excited-state of the alkynyl ligand is not entirely quenched upon addition of 2 equiv of $Er(hfac)_3(H_2O)_2$ (Figure S4, Supporting Information). It appears that energy transfer from the $^1(\pi \rightarrow \pi^*)$ singlet state of the alkynyl ligand in gold(I) chromophores to lanthanide(III) center is not complete even if Au···Ln separation is shorter than 9.0 Å through the bridging 5-ethynyl-2,2′-bipyridine. Consequently, energy transfer from gold(I) alkynyl chromophore to lanthanide(III) center in these Au-Ln arrays (**7**−**14**) is less effective compared with Pt → Ln energy transfer in a series of Pt-Ln heteronuclear species,[6,7] where energy transfer from platinum(II) chromophores to lanthanide centers is always quantitive (complete) when intramolecular Pt···Ln separation is within 10 Å through a bridging polypyridyl ethynyl ligand.[6,7] The less efficient Au → Ln energy transfer in **7**−**14** is probably ascribed to energy mismatching or less spectral overlapping between the emission spectra of gold(I) alkynyl chromophores and the lanthanide(III) absorption spectra from f-f transitions.

Conclusions

A feasible synthetic route is established for preparation of a series of binuclear gold(I) acetylide diphosphine complexes by depolymerizing the polymeric gold(I) species of 5-ethynyl-2,2′-bipyridine using diphosphine ligands. Incorporating the binuclear gold(I) complexes with $Ln(hafc)_3$ units causes formation of the corresponding Au-Ln heteronuclear arrays through 2,2′-bipyridyl chelating the lanthanide(III) centers. Dramatic cis−trans conformational changes occur because of creating or breaking of ligand-support or unsupported Au−Au contacts upon formation of Au_4Ln_4 or Au_2Ln_2 heteronuclear arrays by associating binuclear gold(I) units with $Ln(hafc)_3$ fragments. The binuclear gold(I) complexes show intense luminescence in both solid-states and dichloromethane solutions. At ambient temperature, the high-energy emission arises probably from the intraligand $^1(\pi \rightarrow \pi^*)$ excited-state whereas the low-energy luminescence from $^3(\pi \rightarrow \pi^*)$ triplet state mixed probably with some character from (Au−Au) → (C≡Cbpy) ^{3}MMLCT transition. The excited-state of binuclear gold(I) acetylide phosphine complexes at 77 K is most likely dominated by intraligand $^3(\pi \rightarrow \pi^*)$ state together with some character from the ^{3}MMLCT transition. Sensitized lanthanide luminescence with the lifetimes in microsecond range is successfully achieved in these Au-Ln heteronuclear complexes through efficient Au → Ln energy transfer from the binuclear gold(I) acetylide chromophores to the lanthanide(III) centers.

Experimental Section

Materials and Reagents. The manipulations were carried out under argon atmosphere using Schlenk techniques and vacuum-line systems. The solvents were dried, distilled and degassed prior to use except those for spectroscopic measurements were of spectroscopic grade. 1,2-Bis(diphenylphosphino)ethane (dppe), 1,3-bis(diphenylphosphino)propane (dppp), 1,4-bis(diphenylphosphino)butane (dppb), 1,5-bis(diphenylphosphino)pentane (dpppen), 1,6-bis(diphenylphosphino)hexane (dpph), 1,1′-bis(diphenylphosphino)-ferrocene (dppf), tetrahydrothiophene (tht), and $H_3[AuCl_4]$ were commercially available without purification. 5-[2-(Trimethylsilyl)-1-ethynyl]-2,2′-bipyridine ($bpyC{\equiv}CSiMe_3$),[24] Au(tht)Cl[25] and $Ln(hafc)_3(H_2O)_2$ (Ln = Nd, Eu, Er, Yb)[6c–e] were prepared by the literature procedures.

Caution! *Gold acetylides are potentially explosive and should be handled with care and in small amount.*

$(bpyC{\equiv}CAu)_n$. To a THF (30 mL) solution of Au(tht)Cl (107 mg, 0.344 mmol) was added a methanol (5 mL) solution of potassium fluoride (23 mg, 0.40 mmol). A THF (10 mL) solution of $bpyC{\equiv}CSi(CH_3)_3$ (85.5 mg, 0.344 mmol) was dropwise added to the above solution, producing a bright yellow precipitate with stirring for 3 h. The precipitate was filtered and the yellow solid was washed with THF, methanol, and dichloromethane. Yield: 87%. The solid is insoluble in common organic solvents. IR spectrum (KBr, cm^{-1}): 2006m (C≡C).

$(bpyC{\equiv}CAu)_2(\mu$-dppe) (1). $(bpyC{\equiv}CAu)_n$ (120 mg, 0.32 mmol) was slowly added to a dichloromethane (20 mL) solution of dppe (64 mg, 0.16 mmol) with stirring for 1 h. After filtering, the solution was concentrated and the product was purified by chromatography on a silica gel column using dichloromethane-methanol (100:1) as eluent. Yield: 67%. Anal. Calcd for $C_{50}H_{38}Au_2N_4P_2$: C, 52.19; H, 3.33; N, 4.87. Found: C, 51.86; H, 3.45; N, 4.72. ESI-MS (*m*/*z*): 1151 $[M + H]^+$, 971 $[M\text{-}bpyC{\equiv}C]^+$. ^{1}H NMR ($CDCl_3$, ppm): 8.82 (s, 2H, bpyC≡C), 8.67 (d, 2H, J = 4.0 Hz, bpyC≡C), 8.39 (d, 2H, J = 8.0 Hz, bpyC≡C), 8.33 (d, 2H, J = 8.5 Hz, bpyC≡C), 7.92 (d, 2H, J = 7.5 Hz, bpyC≡C), 7.81 (t, 2H, J = 7.5 Hz, bpyC≡C), 7.50−7.68 (m, 20H, C_6H_5), 7.29 (d, 2H, J = 7.0 Hz, bpyC≡C), 2.68 (s, 4H, CH_2). ^{31}P NMR ($CDCl_3$, ppm): 40.0. IR spectrum (KBr, cm^{-1}): 2102m (C≡C).

(24) Grosshenny, V.; Romero, F. M.; Ziessel, R. J. *Org. Chem.* **1997**, *62*, 1491.
(25) Usón, R.; Laguna, A.; Laguna, M. *Inorg. Synth.* **1989**, *26*, 85.
(26) (a) Hasegawa, Y.; Kimura, Y.; Murakoshi, K.; Wada, Y.; Kim, J.-H.; Nakashima, N.; Yamanaka, T.; Yanagida, S. J. *Phys. Chem.* **1996**, *100*, 10201. (b) Nakamaru, K. *Bull. Chem. Soc. Jpn.* **1982**, *55*, 2697.

(bpyC≡CAu)$_2$(μ-dppp) (2). This compound was prepared by the same synthetic procedure as that of **1** except for using dppp instead of dppe. Yield: 68%. Anal. Calcd for $C_{51}H_{40}Au_2N_4P_2$: C, 52.59; H, 3.46; N, 4.81. Found: C, 52.27; H, 3.62; N, 4.90. ESI-MS (*m*/*z*): 1165 [M + H]$^+$, 985 [M-bpyC≡C]$^+$. ^{1}H NMR ($CDCl_3$, ppm): 8.80 (s, 2H, bpyC≡C), 8.67 (d, 2H, J = 3.5 Hz, bpyC≡C), 8.39 (d, 2H, J = 7.5 Hz, bpyC≡C), 8.33 (d, 2H, J = 8.5 Hz, bpyC≡C), 7.89 (d, 2H, J = 7.5 Hz, bpyC≡C), 7.80 (t, 2H, J = 7.0 Hz, bpyC≡C), 7.45−7.72 (m, 20H, C_6H_5), 7.30 (d, 2H, J = 7.0 Hz, bpyC≡C), 2.86 (m, 4H, CH_2), 1.83 (m, 2H, CH_2). ^{31}P NMR ($CDCl_3$, ppm): 34.9. IR spectrum (KBr, cm^{-1}): 2111m (C≡C).

(bpyC≡CAu)$_2$(μ-dppb) (3). This compound was prepared by the same synthetic procedure as that of **1** except for using dppb instead of dppe. Yield: 68%. Anal. Calcd for $C_{52}H_{42}Au_2N_4P_2\cdot CH_2Cl_2$: C, 50.37; H, 3.51; N, 4.43. Found: C, 49.92; H, 3.68; N, 4.16. ESI-MS (*m*/*z*): 1179 [M + H]$^+$, 999 [M-bpyC≡C]$^+$. ^{1}H NMR ($CDCl_3$, ppm): 8.81 (s, 2H, bpyC≡C), 8.67 (d, 2H, J = 3.5 Hz, bpyC≡C), 8.38 (d, 2H, J = 7.5 Hz, bpyC≡C), 8.32 (d, 2H, J = 8.0 Hz, bpyC≡C), 7.91 (d, 2H, J = 8.5 Hz, bpyC≡C), 7.80 (t, 2H, J = 8.0 Hz, bpyC≡C), 7.48−7.69 (m, 20H, C_6H_5), 7.30 (d, 2H, J = 5.0 Hz, bpyC≡C), 2.43 (m, 4H, CH_2), 1.81 (m, 4H, CH_2). ^{31}P NMR ($CDCl_3$, ppm): 37.6. IR spectrum (KBr, cm^{-1}): 2114m (C≡C).

(bpyC≡CAu)$_2$(μ-dpppen) (4). This compound was prepared by the same synthetic procedure as that of **1** except for using dpppen instead of dppe. Yield: 62%. Anal. Calcd for $C_{53}H_{44}Au_2N_4P_2\cdot CH_3OH$: C, 53.37; H, 3.72; N, 4.70. Found: C, 52.95; H, 4.06; N, 4.52. ESI-MS (*m*/*z*): 1013 [M-bpyC≡C]$^+$. ^{1}H NMR ($CDCl_3$, ppm): 8.80 (s, 2H, bpyC≡C), 8.67 (d, 2H, J = 3.5 Hz, bpyC≡C), 8.38 (d, 2H, J = 7.5 Hz, bpyC≡C), 8.31 (d, 2H, J = 8.0 Hz, bpyC≡C), 7.88 (d, 2H, J = 8.0 Hz, bpyC≡C), 7.80 (t, 2H, J = 7.5 Hz, bpyC≡C), 7.47−7.71 (m, 20H, C_6H_5), 7.29 (d, 2H, J = 4.0 Hz, bpyC≡C), 2.40 (m, 8H, CH_2), 1.81 (m, 2H, CH_2). ^{31}P NMR ($CDCl_3$, ppm): 37.1. IR spectrum (KBr, cm^{-1}): 2112m (C≡C).

(bpyC≡CAu)$_2$(μ-dpph) (5). This compound was prepared by the same synthetic procedure as that of **1** except for using dpph instead of dppe. Yield: 58%. Anal. Calcd for $C_{54}H_{46}Au_2N_4P_2$: C, 53.74; H, 3.84; N, 4.64. Found: C, 53.77; H, 3.99; N, 4.70. ESI-MS (*m*/*z*): 1207 [M + H]$^+$, 1027 [M-bpyC≡C]$^+$. ^{1}H NMR ($CDCl_3$, ppm): 8.79 (s, 2H, bpyC≡C), 8.67 (d, 2H, J = 4.0 Hz, bpyC≡C), 8.38 (d, 2H, J = 8.0 Hz, bpyC≡C), 8.31 (d, 2H, J = 8.5 Hz, bpyC≡C), 7.89 (d, 2H, J = 8.0 Hz, bpyC≡C), 7.80 (t, 2H, J = 7.5 Hz, bpyC≡C), 7.46−7.70 (m, 20H, C_6H_5), 7.29 (d, 2H, J = 7.5 Hz, bpyC≡C), 2.40 (m, 8H, J = 7.5 Hz, CH_2), 1.46 (m, 4H, CH_2). ^{31}P NMR ($CDCl_3$, ppm): 37.8. IR spectrum (KBr, cm^{-1}): 2097m (C≡C).

(bpyC≡CAu)$_2$(μ-dppf) (6). This compound was prepared by the same synthetic procedure as that of **1** except for using dppf instead of dppe. Yield: 70%. Anal. Calcd for $C_{58}H_{42}Au_2N_4FeP_2$: C, 53.31; H, 3.24; N, 4.29. Found: C, 53.15; H, 3.46; N, 4.23. ESI-MS (*m*/*z*): 1306 [M]$^+$, 1127 [M − bpyC≡C]$^+$, 751 [M-Au(bpyC≡C)$_2$]$^+$. ^{1}H NMR ($CDCl_3$, ppm): 8.82 (s, 2H, bpyC≡C), 8.67 (d, 2H, J = 3.5 Hz, bpyC≡C), 8.39 (d, 2H, J = 8.0 Hz, bpyC≡C), 8.32 (d, 2H, J = 8.5 Hz, bpyC≡C), 7.91 (d, 2H, J = 8.0 Hz, bpyC≡C), 7.81 (t, 2H, J = 8.0 Hz, bpyC≡C), 7.43−7.57 (m, 20H, C_6H_5), 7.30 (d, 2H, J = 5.0 Hz, bpyC≡C), 4.76 (s, 4H, C_5H_4), 4.34 (s, 4H, C_5H_4). ^{31}P NMR ($CDCl_3$, ppm): 36.8. IR spectrum (KBr, cm^{-1}): 2111m (C≡C).

{(AuC≡Cbpy)$_2$(μ-dppb)}$_2${Ln(hfac)$_3$}$_4$ (Ln = Nd, Eu, Er, and Yb). The Au_4Ln_4 compounds were prepared by addition of 2.2 equiv of Ln(hfac)$_3$(H_2O)$_2$ to a dichloromethane solution of (bpyC≡CAu)$_2$(μ-dppb) (**3**) with stirring for 1 h. After filtered, the concentrated dichloromethane solutions were layered with *n*-hexane to afford the desired products as pale yellow crystals in 55−70% yields.

7 (Ln = Nd). Yield: 62%. Anal. Calcd. for $C_{164}H_{96}Au_4Nd_4F_{72}N_8O_{24}P_4$: C, 36.35; H, 1.79; N, 2.07. Found: C, 36.59; H, 1.90; N, 2.26. IR spectrum (KBr, cm^{-1}): 2121m (C≡C), 1654s (C═O).

8 (Ln = Eu). Yield: 55%. Anal. Calcd. for $C_{164}H_{96}Au_4Eu_4F_{72}N_8O_{24}P_4$: C, 36.14; H, 1.78; N, 2.06. Found: C, 36.05; H, 1.81; N, 2.16. spectrum (KBr, cm^{-1}): 2121m (C≡C), 1654s (C═O).

9 (Ln = Er). Yield: 68%. Anal. Calcd. for $C_{164}H_{96}Au_4Er_4F_{72}N_8O_{24}P_4$: C, 35.74; H, 1.76; N, 2.03. Found: C, 35.65; H, 1.81; N, 2.03. IR spectrum (KBr, cm^{-1}): 2122m (C≡C), 1652s (C═O).

10 (Ln = Yb). Yield: 70%. Anal. Calcd. for $C_{164}H_{96}Au_4F_{72}N_8O_{24}P_4Yb_4$: C, 35.59; H, 1.75; N, 2.02. Found: C, 35.55; H, 1.80; N, 2.08. IR spectrum (KBr, cm^{-1}): 2122m (C≡C), 1653s (C═O).

{(μ-dppf)(AuC≡Cbpy)$_2$}{Ln(hfac)$_3$}$_2$ (Ln = Nd, Eu, Er, and Yb). These compounds were prepared by the similar synthetic procedures as those of {(AuC≡Cbpy)$_2$(μ-dppb)}$_2${Ln(hfac)$_3$}$_4$ (**7**−**10**) except for using **6** instead of **3.** Yields: 65−80%.

11 (Ln = Nd). Yield: 61%. Anal. Calcd. for $C_{88}H_{52}Au_2Nd_2F_{36}FeN_4O_{14}P_2$: C, 36.82; H, 1.83; N, 1.95. Found: C, 36.93; H, 1.79; N, 1.96. IR spectrum (KBr, cm^{-1}): 2121m (C≡C), 1654s (C═O).

12 (Ln = Eu).Yield: 76%. Anal. Calcd. for $C_{88}H_{52}Au_2Eu_2F_{36}FeN_4O_{14}P_2$: C, 36.54; H, 1.81; N, 1.94. Found: C, 36.43; H, 1.85; N, 1.88. IR spectrum (KBr, cm^{-1}): 2121m (C≡C), 1654s (C═O).

13 (Ln = Er). Yield: 80%. Anal. Calcd. for $C_{88}H_{52}Au_2Er_2F_{36}FeN_4O_{14}P_2$: C, 36.21; H, 1.80; N, 1.92. Found: C, 36.45; H, 1.73; N, 1.92. IR spectrum (KBr, cm^{-1}): 2113m (C≡C), 1657s (C═O).

14 (Ln = Yb).Yield: 65%. Anal. Calcd. for $C_{88}H_{52}Au_2F_{36}FeN_4O_{14}P_2Yb_2$: C, 36.06; H, 1.79; N, 1.91. Found: C, 36.15; H, 1.80; N, 1.92. IR spectrum (KBr, cm^{-1}): 2122m (C≡C), 1653s (C═O).

Physical Measurements. Elemental analyses (C, H, N) were carried out on a Perkin-Elmer model 240C elemental analyzer. Electrospray ion mass spectroscopy (ESI-MS) was performed on a Finnigan LCQ mass spectrometer using dichloromethane-methanol mixture as mobile phases. ^{1}H and ^{31}P NMR spectra were measured on a Varian UNITY-500 spectrometer with $SiMe_4$ as the internal reference and 85% H_3PO_4 as external standard, respectively. UV−vis absorption spectra were measured on a Perkin-Elmer Lambda 25 UV−vis spectrophotometer. Infrared (IR) spectra were recorded on a Magna750 FT-IR spectrophotometer with KBr pellet. Emission and excitation spectra in the UV−vis region were recorded on a Perkin-Elmer LS 55 luminescence spectrometer with a red-sensitive photomultiplier type R928. Emission lifetimes in solid states and degassed solutions were determined on an Edinburgh Analytical Instrument (F900 fluorescence spectrometer) using LED laser at 397 nm excitation and the resulting emission was detected by a thermoelectrically cooled Hamamatsu R3809 photomultiplier tube. The instrument response function at the excitation wavelength was deconvolved from the luminescence decay. Near-infrared (NIR) emission spectra were measured on an Edinburgh FLS920 fluorescence spectrometer equipped with a Hamamatsu R5509-72 supercooled photomultiplier tube at 193 K and a TM300 emission monochromator with NIR grating blazed at 1000 nm. The NIR emission spectra were corrected via a calibration curve supplied with the instrument. The emission quantum yields (Φ) of **1**−**5** in degassed dichloromethane solutions at room temperature were calculated by $\Phi s = \Phi r(B_r/B_s)(n_s/n_r)_2(D_s/D_r)$ using $Cy_3PAuC{\equiv}CPh$ in dichloromethane as the standard ($\Phi_{em} = 0.08$),[22] whereas **8** and **12** using $[Ru(bpy)_3](PF_6)_2$ in acetonitrile as the standard ($\Phi_{em} = 0.062$).[26] The subscripts r and s denote reference standard and the sample solution, respectively; and n, D and Φ are the refractive index of the solvents, the integrated intensity and the luminescence

Table 3. Crystallographic Data of **1**·2CH_2Cl_2, **3**·H_2O, **6**·2H_2O, **9**·H_2O, and **13**·2H_2O

	1·2CH_2Cl_2	**3**·H_2O	**6**·CH_2Cl_2	**9**·H_2O	**13**·2H_2O
empirical formula	$C_{52}H_{42}Au_2Cl_4N_4P_2$	$C_{52}H_{44}Au_2N_4OP_2$	$C_{29.5}H_{22}AuClFe_{0.5}N_2P$	$C_{164}H_{98}Au_4Er_4$ $F_{72}N_8O_{25}P_4$	$C_{44}H_{26}AuErF_{18}Fe_{0.5}N_2O_7P$
fw	1320.57	1196.79	695.80	5529.29	1459.79
space group	$P2_1/c$	$P\bar{1}$	$P2/n$	$P\bar{1}$	$P2/c$
a, Å	16.5112 (11)	13.729(4)	12.8471 (14)	20.572(7)	11.9836 (7)
b, Å	14.4610 (8)	14.146(4)	10.7684 (9)	22.652(7)	28.1903 (13)
c, Å	22.8777 (16)	15.336(4)	18.3317 (16)	26.149(9)	15.4321 (8)
α, °	90.00	69.155 (13)	90.00	65.407 (11)	90.00
β, °	103.144 (3)	66.212 (11)	92.402(6)	87.920 (18)	100.348 (3)
γ, °	90.00	66.377 (11)	90.00	78.729 (15)	90.00
V, Å^3	5319.4 (6)	2429.1 (10)	2533.8(4)	10852(6)	5128.5(5)
Z	4	2	4	2	4
ρ_{calcd} g/cm^{-3}	1.649	1.636	1.824	1.692	1.891
μ, mm^{-1}	5.808	6.139	6.271	4.369	4.763
radiation (λ, Å)	0.71073	0.71073	0.71073	0.71073	0.71073
temp, (K)	293(2)	293(2)	293(2)	293(2)	293(2)
R1 (F_o)	0.0494	0.0526	0.0547	0.0783	0.054
wR2 (F_o^2)	0.1326	0.1386	0.1439	0.1940	0.1453
GOF	1.100	0.945	1.042	1.067	1.058

quantum yield, respectively. The quantity B is calculated by $B = 1 - 10^{-AL}$, where A is the absorbance at the excitation wavelength and L is the optical path length. All the solutions used for determination of emission lifetimes and quantum yields were prepared under a vacuum in a 10 cm^3 round-bottom flask equipped with a sidearm 1 cm fluorescence cuvette and sealed from the atmosphere by a quick-release Teflon stopper. Solutions used for luminescence determination were prepared after rigorous removal of oxygen by three successive freeze−pump−thaw cycles.

Crystal Structural Determination. Crystals suitable for X-ray diffraction were grown by layering *n*-hexane onto the corresponding dichloromethane solutions. Data collection was performed on a RIGAKU MERCURY CCD diffractometer by ω scan technique at room temperature using graphite-monochromated MoKα (λ = 0.71073 Å) radiation. Lp corrections were carried out in the reflection reduction process. The structures were solved by direct method and the heavy atoms were located from E-map. The remaining non-hydrogen atoms were determined from the successive difference Fourier syntheses. The non-hydrogen atoms were refined anisotropically except for the F atoms in **9** and **13**, and the hydrogen atoms were generated geometrically with isotropic thermal parameters. The structures were refined on F^2 by full-matrix least-squares methods using the SHELXTL-97 program package. For **9** and **13**, the refinements were carried out by fixing the C−F distances (1.32 ± 0.01 Å) with the occupancy factors of F1−F36 and F1′-F36′ being 0.50, respectively. Crystallographic data for **1**·2CH_2Cl_2, **3**·H_2O, **6**·2H_2O, **9**·H_2O, and **13**·2H_2O were summarized in Table 3.

Acknowledgment. This work was financially supported by the NSFC (Grants 20521101, 20625101 and 20773128), the 973 project (Grant 2007CB815304) from MSTC, the NSF of Fujian Province (Grants 2006F3131 and 2008I0027), and the fund from the Chinese Academy of Sciences (Grant KJCX2-YW-H01).

Supporting Information Available: Figures giving additional UV−vis absorption and emission spectra, and X-ray crystallographic files in CIF format for the structure determination of compounds **1**·2CH_2Cl_2, **3**·H_2O, **6**·CH_2Cl_2, **9**·H_2O, and **13**·2H_2O. This material is available free of charge via the Internet at http://pubs.acs.org.

IC800733X